Ruthenium-catalyzed [2+2] cycloadditions between substituted alkynes and norbornadiene: a theoretical study

Peng Liu, William Tam and John D. Goddard[*]

Department of Chemistry, University of Guelph, Guelph, Ontario N1G 2W1, Canada

Abstract—Theoretical predictions have been made using density functional theory for the reaction paths of a series of substituted alkynes undergoing a ruthenium-catalyzed cycloaddition with norbornadiene. Substituents on the alkynes have been varied in order to probe electronic and steric effects and the role of an intramolecular hydrogen bond. Strong electron-withdrawing groups activate the alkyne and decrease the reaction barrier leading to an increased rate. Bulkier substituents are predicted to lead to higher barriers and slower rates. The hydroxyl group on the alkyne hydrogen bonds to the chlorine stabilizes the transition state and increases the reaction rate. Generally good agreement is found with the trends in recently reported experimental relative rates of reaction of substituted alkynes with norbornadiene.
© 2007 Elsevier Ltd. All rights reserved.

1. Introduction

Transition metal catalyzed cycloaddition reactions are among the most powerful and most frequently used methods in the synthesis of ring derivatives.[1–3] In most of these cycloaddition reactions, carbon–carbon σ-bond activation by the transition metal catalyst[4,5] is of great importance and has remarkable effects on the reactivity as well as the regio- and stereoselectivity. Obviously, substituents on the alkyne will affect the degree of σ-bond activation and thus the reactivity of the alkyne.[6–9]

In the past decade, ruthenium(II)-catalyzed [2+2] cycloaddition reactions between an alkene and an alkyne have been developed[10–16] as an effective way to construct cyclobutene derivatives. In contrast, only few theoretical investigations of ruthenium-catalyzed [2+2] cycloadditions have been reported.[12,16] Recently, Tam and co-workers showed that alkynes with various substituents exhibit remarkably different reactivities in the catalyzed reaction with norbornadiene[17] (Table 1). Reactivity of the alkyne component increases dramatically as the alkyne becomes more electron deficient, while an increase in the steric bulk of the alkyne decreases the reactivity, and the addition of a propargylic alcohol group greatly increases the reactivity. This theoretical study was carried out to rationalize the influence of substituents on the alkyne on the ruthenium-catalyzed [2+2] cycloaddition reactions. To the best of our knowledge, no theoretical study on the substituent effects on the alkyne σ-bond activation or on the reactivity of the alkyne components has been reported.

Table 1. Relative rates of the reactions of different alkynes with norbornadiene in the ruthenium-catalyzed [2+2] cycloadditions[17]
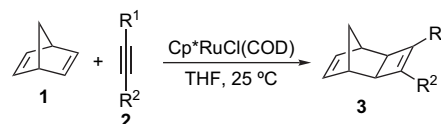
Entry	Alkyne	R_1	R_2	Cycloadduct	Relative rate
1	**2a**	CH_3	Ph	**3a**	<0.0016
2	**2b**	COOH	Ph	**3b**	0.6
3	**2c**	COOEt	Ph	**3c**	1
4	**2d**	COOEt	CH_2OH	**3d**	13
5	**2e**	COOEt	*t*-Bu	**3e**	No reaction
6	**2f**	COOEt	*c*-Hexyl	**3f**	0.03
7	**2g**	COOEt	*n*-Bu	**3g**	0.2
8	**2h**	COOEt	CMe_2OH	**3h**	0.2
9	**2i**	COOEt	CHMeOH	**3i**	5.6
10	**2j**	CH_2OH	Ph	**3j**	<0.04

2. Computational details

All computations were performed with the Gaussian 98[18] or Gaussian 03[19] software packages. The Becke three-parameter hybrid functional[20] combined with the Lee, Yang, and Parr (LYP) correlation functional,[21] B3LYP, was used. Density functional theory clearly improves on Hartree–Fock for the structures and energetics of intermediates and transition states at modest computational cost. Higher level methods such as coupled cluster are prohibitively expensive given the size of the molecules and the number of structures to be computed. B3LYP with reasonable size basis sets is likely to be semi-quantitatively accurate and to allow rationalization of the observed experimental trends.

---

* Corresponding author. E-mail: jgoddard@uoguelph.ca

The LACVP* basis set, which uses the Los Alamos effective core potential plus a double-zeta basis set LANL2DZ[22] on ruthenium and the 6-31G(d) basis set[23–27] for the remaining atoms was employed. All structures have closed-shell electronic states. Isolated molecules were considered without the inclusion of solvent and thus differential salvation of structures along the profiles is neglected. Such an approximation could be tested with further extensive computations including salvation by a continuum model. Harmonic vibrational frequencies were computed to verify the nature of stationary points. All transition-state (TS) structures were characterized by one imaginary frequency, which defines them as first-order saddle points. To better ascertain that the transition states link the expected products and reactants, the normal mode corresponding to the imaginary frequency was animated and observed closely. All reactant and product structures had no imaginary vibrational frequencies and are minima. The harmonic vibrational frequencies are used to correct all reported energies to include the zero point vibrational energy (ZPVE). Natural Population Analysis (NPA) charges were obtained with the NBO program[28] in Gaussian 98.

3. Results and discussion

A proposed mechanism for the ruthenium-catalyzed [2+2] cycloadditions between norbornadiene and alkynes is shown in Figure 1. Dissociation of the cyclooctadiene (COD) 10 from the catalyst Cp*RuCl(COD) 4 (Cp*=pentamethyl-cyclopentadiene, C_5Me_5) followed by complexation with alkyne 2 and norbornadiene 1 produces the ruthenium π-complex 6. Since all cycloadducts obtained experimentally are *anti-exo*, in all the theoretical studies, we focused only on those complexes where the ruthenium is attached to the *anti-π* bond on the *exo* face of the norbornadiene. There are four ways to arrange the four different groups (Cl, Cp*, norbornadiene 1, and alkyne 2), which are attached

to ruthenium (see Fig. 2). Previous studies of 7-substituted norbornadienes have shown[12] that among the four different arrangements, the structure in which the Cl is located above C_6, the alkyne above C_5, and the Ru–Cp* bond is coplanar with the C_7–H_7 bond of the norbornadiene has the lowest energy. (The numbering of the relevant carbons was presented in Fig. 2.) The arrangement is favored in all reactions examined previously in the rate-determining oxidative addition step.[12] Focusing on this preferred arrangement, there are two ruthenium π-complex structures due to different orientations of the unsymmetrically substituted alkyne 2. The relative stability of these two structures obviously will be affected by the electronic and steric properties of the substituents R_1 and R_2. These two complexes lead to the two different pathways (A and B), which will be examined.

#### 3.1. Electronic effects of the substituents

To gain insight into the detailed reaction mechanism and especially the effect of substituents on the alkyne on the reaction, computational studies of the potential energy profiles of the reaction between norbornadiene 1 and four alkynes: 2a (R_1=CH$_3$, R_2=Ph), 2b (R_1=COOH, R_2=Ph), 2c (R_1=COOEt, R_2=Ph), and 2d (R_1=COOEt, R_2= CH$_2$OH) were carried out.

The predicted potential energy profiles of pathways A and B for the reaction between norbornadiene 1 and alkyne 2a (R_1=CH$_3$, R_2=Ph) are shown in Figure 3; the numbers in bold are the relative energies with respect to the separated reactants (norbornadiene 1, alkyne 2a, and the catalyst Cp*RuCl(COD) 4); the numbers in italics are the energy differences between different structures along the reaction coordinate.
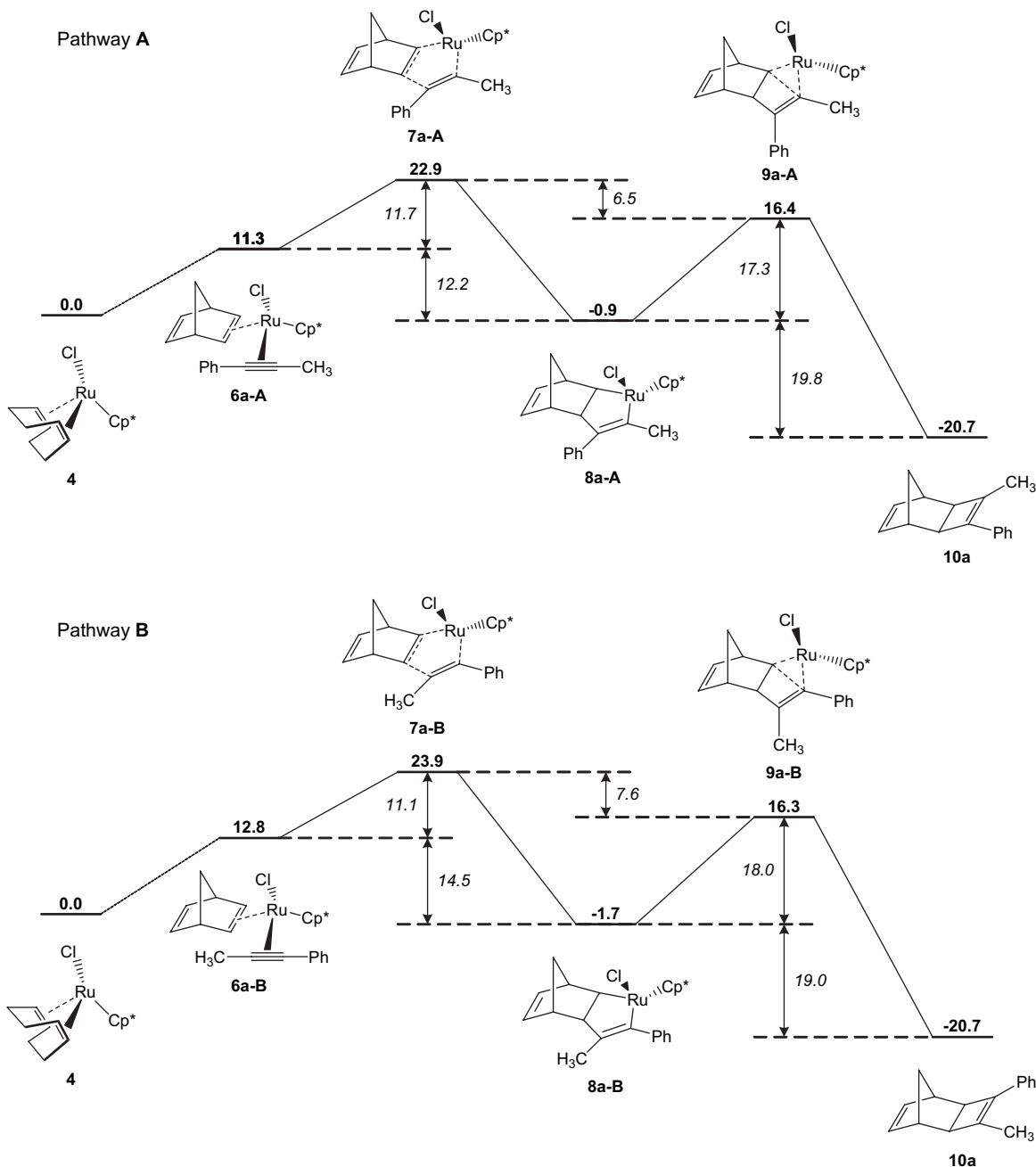
In pathway A of this reaction, the activation energy for oxidative addition from the ruthenium π-complex 6a-A to the
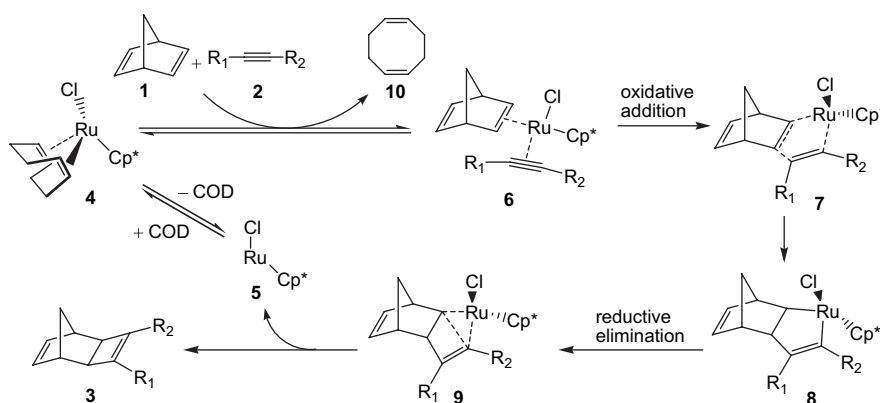
Figure 1. Proposed mechanism for the ruthenium-catalyzed [2+2] cycloaddition between norbornadiene 1 and alkynes 2.

Preferred Arrangement
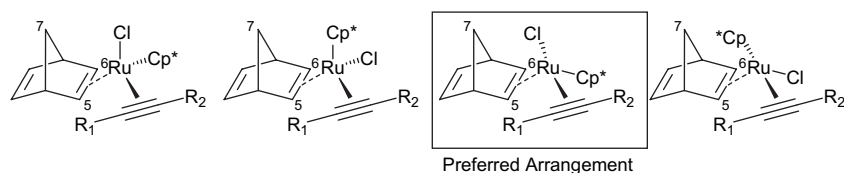
Figure 2. Four possible arrangements of the groups connected to ruthenium.
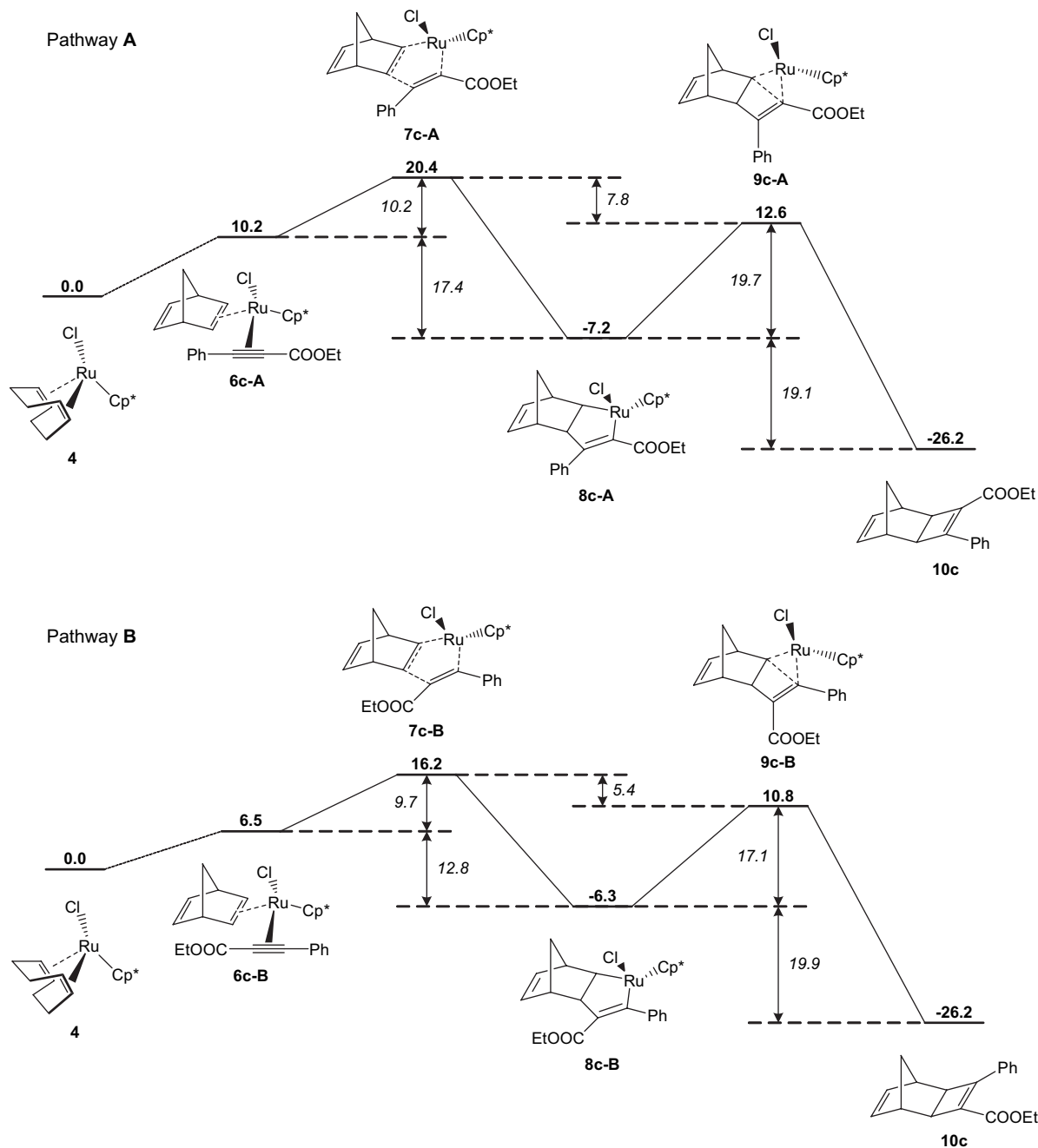
Pathway **A**

Pathway **B**

Figure 3. Potential energy profiles for pathways **A** and **B** of the ruthenium-catalyzed [2+2] cycloaddition between norbornadiene **1** and alkyne **2a** (R_1=CH$_3$, R_2=Ph). Energy differences in kcal/mol.

first transition state **7a-A** is 11.7 kcal/mol, and for the resulting metallacyclopentene **8a-A** is 12.2 kcal/mol, which is more stable than **6a-A**. The activation energy for the reductive elimination of **8a-A** to the second transition state **9a-A** (17.3 kcal/mol) is higher than the first step, however, the energy of the second transition state is 6.5 kcal/mol, which is lower than the first transition state. The resulting cycloadduct **10a-A** and regenerated Cp*RuCl are 19.8 kcal/mol more stable than the metallacycle **8a-A**.

For pathway **B**, the energy barriers and relative energies are quite similar to pathway **A**. The electronic effects due to the phenyl and methyl groups are similar, thus similarities in energetics would be expected. The products of the two

pathways **10a-A** and **10a-B** are optical isomers and have the same energies relative to reactants.

By replacing the CH$_3$ group in alkyne **2a** with a strong electron-withdrawing group, COOEt, the C–C bond in the alkyne **2c** is polarized. This polarization causes the different reactivities for pathways **A** and **B**. The predicted potential energy profiles of these two pathways for the reaction between alkyne **2c** and norbornadiene **1** are shown in Figure 4. From these potential energy profiles, we see clearly the energy differences between pathways **A** and **B**. For the ruthenium π-complex and the first transition state, pathway **A** requires approximately 4 kcal/mol more energy than pathway **B**. The metallacyclopentene intermediates have

Pathway **A**

Pathway **B**

Figure 4. Potential energy profiles for pathways **A** and **B** of the ruthenium-catalyzed [2+2] cycloaddition between norbornadiene **1** and alkyne **2c** (R_1=COOEt, R_2=Ph). Energy differences in kcal/mol.

comparable energies for the two pathways. In the reductive elimination step, the activation energy for pathway **A** is 2.6 kcal/mol, greater than that of pathway **B**. Qualitatively similar potential energy profiles (PRC to the TS for addition then on to the metallacycle intermediate and the elimination TS to bicyclic product) of pathways **A** and **B** for alkynes **2b** and **2d** are shown in Figures S1 and S2 in Supplementary data. Note a significant difference for pathway **B** of alkyne **2d** where the initial complex lies lower in energy than the reactants effectively increasing the first barrier to 8.6 kcal/mol. The increase in relative rate from ∼1 for **2b** and **2c** to only 13 is more readily understood if the barrier versus the complex is used in the exceptional case of **2d**.

Having determined these potential energy profiles for reactions with the different alkynes, two important questions arise: (i) what in the potential energy profiles determines the reaction rates? (ii) How do substituents on the alkyne change this factor? The steady state approximation suggests that the main factor affecting the overall reaction rate is the relative energy of the first transition state with respect to the reactants and thus a lower energy oxidative addition transition states lead to a faster reaction. In a simple explanation, the first transition state has the highest energy in the entire potential energy profile. Thus, it would be the rate-determining step along the reaction coordinate. This is in agreement with our earlier theoretical studies of ruthenium-catalyzed [2+2]

Table 2. Predicted relative energies of the first transition states **7a–7d** with respect to separated reactants

Entry	Alkyne	R_1	R_2	E (kcal/mol)			Relative rate
				Pathway **A**	Pathway **B**	Favored pathway	Ref. [17]
1	**2a**	CH_3	Ph	22.9	23.9	22.9	<0.0016
2	**2b**	COOH	Ph	15.1	15.6	15.1	0.6
3	**2c**	COOEt	Ph	20.4	16.2	16.2	1
4	**2d**	COOEt	CH_2OH	10.0	2.6	2.6	13

cycloadditions between 2-substituted norbornenes and alkynes.[16] The relative energies of the first transition states are given in Table 2. The predicted stability of the first transition state parallels the experimental relative rate with the exception of **2b**, which is considered further in Section 3.3.

To obtain a greater understanding of the alkyne substituent effect, Natural Population Analysis (NPA) was performed on the first transition state structures **7a–7d**. The calculated NPA charges of the alkyne carbons C_a and C_b and of the C_5 and C_6 carbons in norbornadiene are listed in Table 3. Due to the transition metal induced polarization effect on the alkene C_5–C_6 bond, C_5 is more positive than C_6. (The numbering of the carbons is given in Fig. 2.) For the alkynes **2b–2d**, the strong electron-withdrawing group R_1 (COOEt or COOH) polarizes the alkyne C_a–C_b bond. C_a is more negative than C_b. In the oxidative addition step, pathway **A** forms the C_b–C_5 bond, and pathway **B** forms the C_a–C_5 bond. Thus, the oxidative addition transition state is more stable in pathway **B** than in pathway **A** due to an electronic effect. Pathway **B** is the favored one. For the unactivated alkyne **2a**, the charge difference between C_a and C_b is small for both pathways (0.09 and −0.06). Thus, pathways **A** and **B** would be expected to have similar energies in the oxidative cyclization transition states (11.3 and 12.8 kcal/mol) and similar reactivities.

3.2. Steric effects due to the substituents

To study the steric effects of the substituents on the reactivities of the alkynes, structures of the rate-determining oxidative cyclization transition states **7** of both pathways for
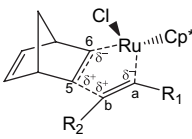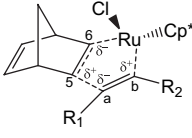
additional reactions with different substituents on the alkynes were studied (**2e**: R_1=COOEt, R_2=*t*-Bu; **2f**: R_1=COOEt, R_2=*c*-hexyl; **2g**: R_1=COOEt, R_2=*n*-Bu; **2h**: R_1=COOEt, R_2=CMe_2OH; and **2i**: R_1=COOEt, R_2=CHMeOH). The predicted energy differences of these structures are presented in Table 4.

By replacing the tertiary carbon *t*-Bu group with a smaller secondary carbon group *c*-hexyl, these two activation energies were reduced from 26.7 to 20.6 kcal/mol for pathway **A** and from 20.5 to 16.4 kcal/mol for pathway **B**. Among the aryl and alkyl substituted alkynes tested (**7e**: R_2=*t*-Bu, **7f**: R_2=*c*-hexyl, **7g**: R_2=*n*-Bu, and **7c** R_2=Ph, entries 1–4 in Table 4), the predicted energy barriers with the primary *n*-Bu substituents (**7g**) are the lowest. For these four alkynes, the differences in activation energies between pathways **A** and **B** fall in the range of 4–6 kcal/mol. Steric repulsions have similar effects on both pathways.

Results on **7h**, **7i**, and **7d** (entries 5–7 in Table 4) illustrate the steric effects of substituents containing an OH group. All these three compounds have much lower activation energies than entries 1–4 without the OH group. Among entries 5–7, the activation energies decrease as R_2 becomes smaller. This is in agreement with the trend in the experimental relative rates.

The theoretical predictions indicate that alkynes with bulkier substituents have higher activation energies for both pathways in the rate-determining step involving oxidative cyclization. This prediction is in agreement with experiment: alkynes with bulkier substituent react more slowly.

Table 3. Predicted NPA charges of the alkyne carbon C_a and C_b and the alkene carbons C_5 and C_6 in the oxidative addition transition-state structures **7a–7d**

Alkyne	R_1	R_2	C_5	C_6	C_5 minus C_6	C_a	C_b	C_b minus C_a

Pathway **A**

2a	CH_3	Ph	−0.222	−0.270	0.048	0.019	−0.069	−0.088
2b	COOH	Ph	−0.226	−0.272	0.046	−0.174	0.018	0.192
2c	COOEt	Ph	−0.229	−0.261	0.032	−0.131	−0.008	0.123
2d	COOEt	CH_2OH	−0.233	−0.264	0.031	−0.127	−0.038	0.089

Pathway **B**

2a	CH_3	Ph	−0.238	−0.262	0.024	−0.022	0.042	−0.064
2b	COOH	Ph	−0.193	−0.267	0.074	−0.220	0.069	−0.289
2c	COOEt	Ph	−0.203	−0.255	0.052	−0.203	0.054	−0.257
2d	COOEt	CH_2OH	−0.206	−0.266	0.060	−0.195	0.036	−0.231

Table 4. Predicted relative energies of the first transition states **7a–7j** with respect to reactants

| Entry	Structure	R_1	R_2	ΔE (kcal/mol)			Relative rate from experiment[17]
				Pathway **A**	Pathway **B**	Favored pathway	
1	**7e**	COOEt	*t*-Bu	26.7	20.5	20.5	No reaction
2	**7f**	COOEt	*c*-Hexyl	20.6	16.4	16.4	0.03
3	**7g**	COOEt	*n*-Bu	19.6	14.1	14.1	0.2
4	**7c**	COOEt	Ph	20.4	16.2	16.2	1
5	**7h**	COOEt	CMe_2OH	18.2	6.3	6.3	0.2
6	**7i**	COOEt	$CHMeOH$	12.5	3.5	3.5	5.6
7	**7d**	COOEt	CH_2OH	10.0	2.6	2.6	13
8	**7a**	CH_3	Ph	22.9	23.9	22.9	<0.0016
9	**7j**	CH_2OH	Ph	13.9	21.3	13.9	<0.04
10	**7b**	COOH	Ph	15.1	15.6	15.1	0.6

3.3. Intramolecular hydrogen bond

Intramolecular hydrogen bonds may stabilize the reactants or transition state structures and affect the reactivities. Previous studies showed that M–Cl moieties (M=transition metal) are good, anisotropic hydrogen bond acceptors forming such bonds with similar lengths to those involving the chloride anion.[29]

For the reaction pathways in which the Cp*RuCl is close to a hydroxyl group (OH) on the alkyne, an intramolecular

chlorine–hydrogen interaction is predicted to occur for the ruthenium π-complex, the metallacyclopentene, and both of the transition states. Among the reaction pathways studied, pathway **A** for alkyne **2b** (R_1=COOH, R_2=Ph), pathway **B** for alkyne **2d** (R_1=COOEt, R_2=CH_2OH), **2i** (R_1=COOEt, R_2=CHMeOH), and **2h** (R_1=COOEt, R_2=CMe_2OH) contain these hydrogen bonds.

The chlorine–hydrogen interactions in pathway **B** of the reaction with alkyne **2d** (R_1=COOEt, R_2=CH_2OH) are illustrated in Figure 5. A twisted six-membered ring
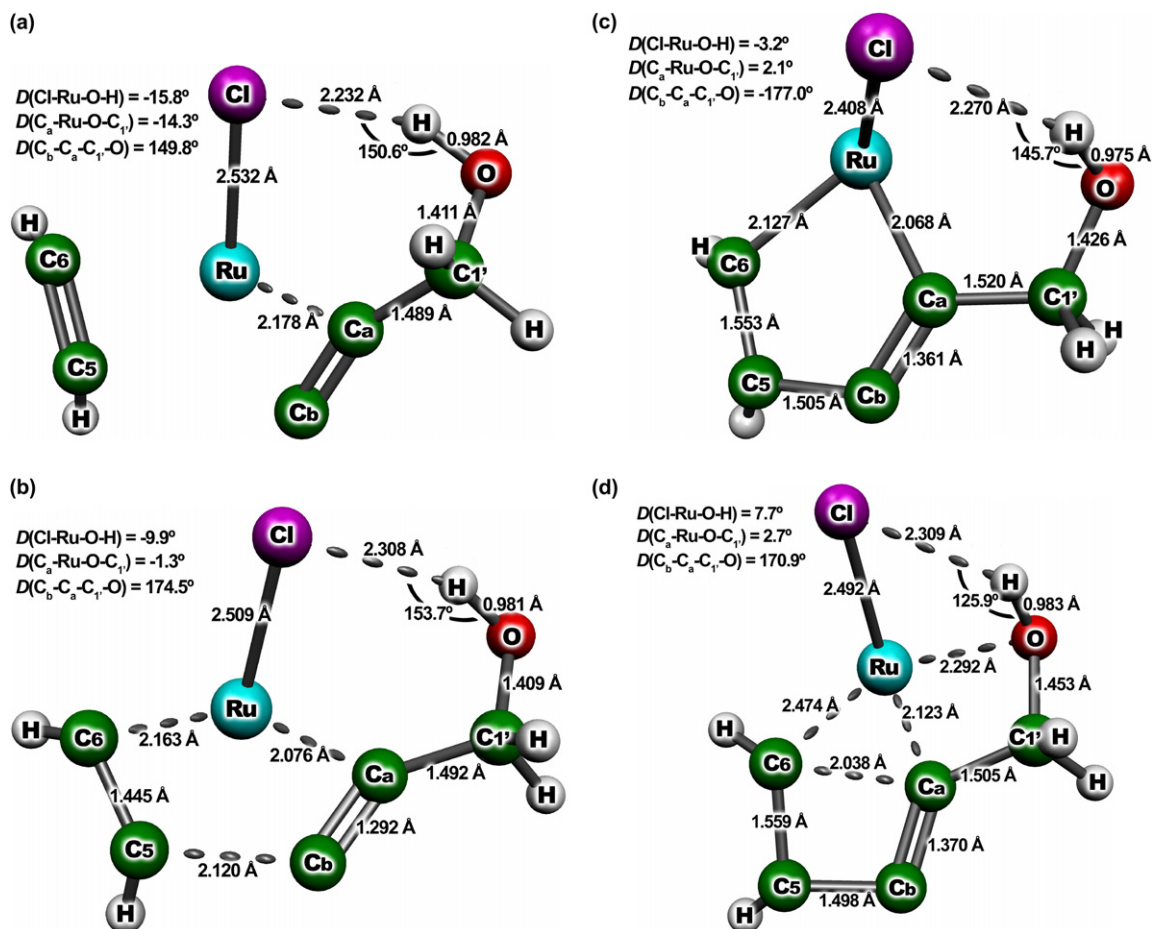
Figure 5. Intramolecular Cl···H hydrogen bonds in the structures on pathway **B** of the reaction between norbornadiene **1** and alkyne **2d** (R_1=COOEt, R_2=CH_2OH). Reaction center (a) as taken from the pre-reaction π-complex **6d-B**, (b) as taken from the oxidative cyclization transition state **7d-B**, (c) as taken from the metallacyclopentene **8d-B**, and (d) as taken from the reductive elimination transition state **9d-B**.

(Cl–Ru–C$_a$–C$_{1'}$–O–H) is formed. The most stable conformer has a butterfly conformation with two nearly planar four-membered rings. The Cl, Ru, O, and H atoms are almost in the same plane. (The dihedral angles D(Cl–Ru–O–H) are $-15.8°$, $-9.9°$, $-3.2°$, and $7.7°$ for **6d-B** to **9d-B**, respectively). C$_a$, Ru, O, and C$_{1'}$ also are in nearly the same plane. (The dihedral angles D(C$_a$–Ru–O–C$_{1'}$) are $-14.3°$, $-1.3°$, $2.1°$, and $2.7°$ for **6d-B** to **9d-B**, respectively).

A short Ru–O distance (2.29 Å) was predicted in the reductive elimination transition state **9d-B**. This interaction stabilizes a transition state, which is not involved in the rate-determining step. As such, it will not obviously affect the reactivity. The chlorine–hydrogen distances r(Cl–H) and bond angles Cl–H–O for the structures in the other reactions are summarized in Table 5. For a better understanding of this interaction, optimized structures in pathway **A** for the reaction with alkene **2j** (R$_1$=CH$_2$OH, R$_2$=Ph) also are given.

Except for **8b-A**, the reductive elimination transition state of pathway **A** for alkyne **2b**, the chlorine–hydrogen distances fall in the range of 2.0–2.4 Å, less than the sum of the hydrogen and chlorine van der Waals radii,[30] which is 2.95 Å. The Cl–H–O bond angles vary from 125° to 170°.

To study stabilization effect of the hydrogen bond, the energy profiles of pathway **A** for the cycloaddition of alkyne **2a** (R$_1$=CH$_3$, R$_2$=Ph, Fig. 3), **2j** (R$_1$=CH$_2$OH, R$_2$=Ph, Fig. S3), **2c** (R$_1$=COOEt, R$_2$=Ph, Fig. 4) and **2b** (R$_1$=COOH, R$_2$=Ph, Fig. S1) are compared. The predicted energies for the structures in these pathways are summarized in Table 7. Table 6 summarizes the NPA charges of the alkynes **2a**, **2j**, **2c**, and **2b**. With the CH$_3$ and the CH$_2$OH groups, no strong carbon–carbon bond polarization exists in the alkynes, **2a** or **2j**. However, the stabilities of the structures along the reaction coordinate are quite different for alkynes **2a** and **2j** (Table 7). The pre-reaction π-complexes, metallacycles and the two transition states, **6j–9j** are about 8–10 kcal/mol more stable than **6a–9a**, respectively. Hydrogen bonding by the OH group is implicated.

The electronegativities of COOEt and COOH are similar and the C$_a$–C$_b$ bonds in alkynes **2c** and **2b** have comparable degrees of polarization (Table 6, last two columns). Due to the stabilization by the hydrogen bond in structures **6c-A** to **8c-A**, the pre-reaction complex **6c-A**, oxidative cyclization transition state **7c-A**, and metallacycle **8c-A** are 5–8 kcal/mol more stable than **6b-A**, **7b-A**, and **8b-A**, respectively. These energy differences are smaller than those caused by the hydrogen bond from the CH$_2$OH group of alkyne **2j**.

Table 6. Predicted NPA charges on carbons C$_a$ and C$_b$ and differences in the charges on C$_a$ and C$_b$ of the alkynes **2a**, **2j** and **2c**, **2b**

$$R_2—C_b{\equiv}C_a—R_1$$

Alkyne	R$_1$	R$_2$	C$_a$	C$_b$	C$_a$ minus C$_b$
2a	CH$_3$	Ph	0.019	−0.038	0.057
2j	CH$_2$OH	Ph	0.010	−0.003	0.013
2c	COOEt	Ph	−0.093	0.058	0.151
2b	COOH	Ph	−0.109	0.069	0.178

Table 7. Predicted energies (relative to reactants, in kcal/mol) for the structures on pathway **A** for the cycloadditions of alkynes **2a** and **2j** and **2c** and **2b**

E (A)	R$_1$	R$_2$	6	7	8	9
Alkyne **2a**	CH$_3$	Ph	11.3	22.9	−0.9	16.4
Alkyne **2j**	CH$_2$OH	Ph	1.8	13.9	−9.0	6.5
ΔE (A, **2a–2j**)			9.5	9.0	8.1	9.9
Alkyne **2c**	COOEt	Ph	10.2	20.4	−7.2	12.6
Alkyne **2b**	COOH	Ph	2.5	15.1	−12.3	12.0
ΔE (A, **2c–2b**)			7.7	5.3	5.1	0.6

As no hydrogen bond interaction is found in the reductive elimination transition state **9c-A** (Table 5), the energy difference between **9c-A** and **9b-A** is quite small (0.6 kcal/mol).

For alkynes **2b** and **2j** containing OH groups, due to the stabilization by the hydrogen bond, the energies of the oxidative cyclization transition states for pathway **A** are even lower than those of pathway **B**, making pathway **A** favored (Table 4). For other pathways with the chlorine–hydrogen interaction listed in Table 5, pathway **B** for alkynes **2d**, **2i**, and **2h**, extremely low activation energies are found from the reactants to the oxidative cyclization transition states (Table 4), making the reactions of alkynes with an OH group at the α-position very fast.

The overall energetics of the hydrogen bonding would be modified (reduced strength of the intramolecular interaction) if solvent effects were included. Hydrogen bonds to solvent molecules such as THF would need to be broken at a cost in energy prior to forming the intramolecular hydrogen bonds.

4. Conclusions

We have reported the first theoretical studies of the reactivity of the alkyne component in ruthenium-catalyzed [2+2] cycloadditions between norbornadiene and substituted alkynes. The large differences in reactivity of the alkyne components are due to substituent effects. The theoretical

Table 5. Chlorine–hydrogen bond distances and Cl⋯H–O bond angles in the reaction pathways where intramolecular Cl⋯H interactions exist

Alkyne	R$_1$	R$_2$	Pathway	π-Complex	First transition state	Metallacycle	Second transition state
2b	COOH	Ph	**A**	2.05 Å	2.13 Å	2.19 Å	2.88 Å
				168.5°	168.4°	152.0°	92.6°
2d	COOEt	CH$_2$OH	**B**	2.23 Å	2.31 Å	2.27 Å	2.31 Å
				150.6°	153.7°	145.7°	125.9°
2i	COOEt	CHMeOH	**B**	2.20 Å	2.31 Å	2.22 Å	2.35 Å
				155.3°	154.3°	126.8°	121.0°
2h	COOEt	CMe$_2$OH	**B**	2.23 Å	2.28 Å	2.25 Å	2.31 Å
				156.0°	156.2°	125.0°	122.5°
2j	CH$_2$OH	Ph	**A**	2.22 Å	2.30 Å	2.32 Å	2.25 Å
				148.4°	153.5°	146.5°	128.7°

predictions of the relative rate of different alkynes in the ruthenium-catalyzed [2+2] cycloadditions with norbornadiene indicate that bulkier substituents will decrease the reactivity of alkyne, and strong electron-withdrawing groups on the alkyne will increase the C–C bond polarization and activate the alkyne. An intramolecular hydrogen bonding interaction was observed between the chlorine in the catalyst and the hydroxyl alkyne substituents. This interaction stabilizes the corresponding transition-state structure and increases the reaction rate of alkyne.

Acknowledgements

Supplementary data

Supplementary data associated with this article can be found in the online version, at doi:10.1016/j.tet.2007.05.030.

References and notes

1. Lautens, M.; Klute, W.; Tam, W. *Chem. Rev.* **1996**, *96*, 49.
2. Wender, P. A.; Love, J. A. *Advances in Cycloaddition*; JAI: Greenwich, 1999; Vol. 5.
3. Hegedus, L. S. *Coord. Chem. Rev.* **1997**, *161*, 129.
4. Murai, S. *Activation of Unreactive Bonds and Organic Synthesis*; Springer: Berlin; New York, NY, 1999.
5. Jun, C. H. *Chem. Soc. Rev.* **2004**, *33*, 610.
6. Villeneuve, K.; Riddell, N.; Jordan, R. W.; Tsui, G. C.; Tam, W. *Org. Lett.* **2004**, *6*, 4543.
7. Kitamura, T.; Sato, Y.; Mori, M. *Adv. Synth. Catal.* **2002**, *344*, 678.
8. Yamamoto, Y.; Arakawa, T.; Ogawa, R.; Itoh, K. *J. Am. Chem. Soc.* **2003**, *125*, 12143.
9. Yamamoto, Y.; Okuda, S.; Itoh, K. *Chem. Commun.* **2001**, 1102.
10. Mitsudo, T.; Naruse, H.; Kondo, T.; Ozaki, Y.; Watanabe, Y. *Angew. Chem., Int. Ed. Engl.* **1994**, *33*, 580.
11. Tenaglia, A.; Giordano, L. *Synlett* **2003**, 2333.
12. Jordan, R. W.; Khoury, P. R.; Goddard, J. D.; Tam, W. *J. Org. Chem.* **2004**, *69*, 8467.
13. Jordan, R. W.; Tam, W. *Tetrahedron Lett.* **2002**, *43*, 6051.
14. Jordan, R. W.; Tam, W. *Org. Lett.* **2001**, *3*, 2367.
15. Jordan, R. W.; Tam, W. *Org. Lett.* **2000**, *2*, 3031.
16. Liu, P.; Jordan, R. W.; Kibbee, S. P.; Goddard, J. D.; Tam, W. *J. Org. Chem.* **2006**, *71*, 3793.
17. Jordan, R. W.; Villeneuve, K.; Tam, W. *J. Org. Chem.* **2006**, *71*, 5830.
18. Frisch, M. J.; Trucks, G. W.; Schlegel, H. B.; Scuseria, G. E.; Robb, M. A.; Cheeseman, J. R.; Zakrzewski, V. G.; Montgomery, J. A., Jr.; Stratmann, R. E.; Burant, J. C.; Dapprich, S.; Millam, J. M.; Daniels, A. D.; Kudin, K. N.; Strain, M. C.; Farkas, O.; Tomasi, J.; Barone, V.; Cossi, M.; Cammi, R.; Mennucci, B.; Pomelli, C.; Adamo, C.; Clifford, S.; Ochterski, J.; Petersson, G. A.; Ayala, P. Y.; Cui, Q.; Morokuma, K.; Salvador, P.; Dannenberg, J. J.; Malick, D. K.; Rabuck, A. D.; Raghavachari, K.; Foresman, J. B.; Cioslowski, J.; Ortiz, J. V.; Baboul, A. G.; Stefanov, B. B.; Liu, G.; Liashenko, A.; Piskorz, P.; Komaromi, I.; Gomperts, R.; Martin, R. L.; Fox, D. J.; Keith, T.; Al-Laham, M. A.; Peng, C. Y.; Nanayakkara, A.; Challacombe, M.; Gill, P. M. W.; Johnson, B.; Chen, W.; Wong, M. W.; Andres, J. L.; Gonzalez, C.; Head-Gordon, M.; Replogle, E. S.; Pople, J. A. *Gaussian 98, Revision A.11*; Gaussian: Pittsburgh, PA, 2001.
19. Frisch, M. J.; Trucks, G. W.; Schlegel, H. B.; Scuseria, G. E.; Robb, M. A.; Cheeseman, J. R.; Montgomery, J. A., Jr.; Vreven, T.; Kudin, K. N.; Burant, J. C.; Millam, J. M.; Iyengar, S. S.; Tomasi, J.; Barone, V.; Mennucci, B.; Cossi, M.; Scalmani, G.; Rega, N.; Petersson, G. A.; Nakatsuji, H.; Hada, M.; Ehara, M.; Toyota, K.; Fukuda, R.; Hasegawa, J.; Ishida, M.; Nakajima, T.; Honda, Y.; Kitao, O.; Nakai, H.; Klene, M.; Li, X.; Knox, J. E.; Hratchian, H. P.; Cross, J. B.; Bakken, V.; Adamo, C.; Jaramillo, J.; Gomperts, R.; Stratmann, R. E.; Yazyev, O.; Austin, A. J.; Cammi, R.; Pomelli, C.; Ochterski, J. W.; Ayala, P. Y.; Morokuma, K.; Voth, G. A.; Salvador, P.; Dannenberg, J. J.; Zakrzewski, V. G.; Dapprich, S.; Daniels, A. D.; Strain, M. C.; Farkas, O.; Malick, D. K.; Rabuck, A. D.; Raghavachari, K.; Foresman, J. B.; Ortiz, J. V.; Cui, Q.; Baboul, A. G.; Clifford, S.; Cioslowski, J.; Stefanov, B. B.; Liu, G.; Liashenko, A.; Piskorz, P.; Komaromi, I.; Martin, R. L.; Fox, D. J.; Keith, T.; Al-Laham, M. A.; Peng, C. Y.; Nanayakkara, A.; Challacombe, M.; Gill, P. M. W.; Johnson, B.; Chen, W.; Wong, M. W.; Gonzalez, C.; Pople, J. A. *Gaussian 03, Revision C.02*; Gaussian: Wallingford, CT, 2004.
20. Becke, A. D. *J. Chem. Phys.* **1993**, *98*, 5648.
21. Lee, C.; Yang, W.; Parr, R. G. *Phys. Rev. B* **1988**, *37*, 785.
22. Hay, P. J.; Wadt, W. R. *J. Chem. Phys.* **1985**, *82*, 299.
23. Ditchfield, R.; Hehre, W. J.; Pople, J. A. *J. Chem. Phys.* **1971**, *54*, 724.
24. Hehre, W. J.; Ditchfield, R.; Pople, J. A. *J. Chem. Phys.* **1972**, *56*, 2257.
25. Hariharan, P. C.; Pople, J. A. *Theor. Chim. Acta* **1973**, *28*, 213.
26. Hariharan, P. C.; Pople, J. A. *Mol. Phys.* **1974**, *27*, 209.
27. Gordon, M. S. *Chem. Phys. Lett.* **1980**, *76*, 163.
28. Glendening, E. D.; Reed, A. E.; Carpenter, J. E.; Weinhold, F. NBO, Version 3.1.
29. Aullon, G.; Bellamy, D.; Brammer, L.; Bruton, E. A.; Orpen, A. G. *Chem. Commun.* **1998**, 653.
30. Bondi, A. *J. Phys. Chem.* **1964**, *68*, 441.